Improving EV Lateral Dynamics Control Using Infinity Norm Approach with Closed-form Solution

Alexander Viehweider
Dept. of Advanced Energy
The University of Tokyo, 5-1-5
Kashiwanoha, Kashiwa, Chiba, Japan
Email: viehweider@ieee.org

Valerio Salvucci, Yoichi Hori, Takafumi Koseki
Dept. of Electrical Engineering
University of Tokyo, 3-7-1
Hongo Bunkyoku Tokyo, Japan
Email: valerio@koseki.t.u-tokyo.ac.jp, hori@k.u-tokyo.ac.jp, takafumikoseki@ieee.org

***Abstract*—Over-actuated EVs offer a high degree of freedoms that can be exploited for better vehicle dynamic behaviour, energy efficiency, vehicle safety and comfort. If the cost of the actuators can be brought to a reasonable level, then sophisticated control algorithm should make the most out of the over-actuation property.**

A key aspect in lateral dynamics control of an over actuated EV with In Wheel motors and active front and/or rear steering is the so called control allocation problem. Often such problems are solved using the 2 norm (weighted least square solution) as it is expressed in a closed form-solution and has a low fixed number of arithmetic operations suited for real time control. In this work a closed-form solution based on the infinity norm for the case of 2 to 3 control allocation problem in EV lateral dynamic control is derived, and validated by means of simulation runs considering an electric vehicle with In-Wheel-Motor traction and active front and rear steering. During a "sine with a dwell" steering command at a constant velocity the superiority of the proposed algorithm based on the infinity norm is shown.

I. Introduction

Over-actuated systems have an intrinsic redundancy exploited for fault robustness and in the case that all actuators work properly for optimizing some other property of the system (energy consumption, limiting maximal actuator power ...). They appear in nearly all engineering disciplines. Mechatronic examples are airplanes [1], bi-articularly actuated robots [2], and electric vehicles with In-Wheel-Motors [3] with/without active front and rear steering [4], [5].

As a consequence of redundancy in actuation, a control allocation problem arises in all these applications. Traditionally the 2 norm is used to resolve such problem, due to the fact that it allows to write a solution in a closed form solution. For certain specific problems, such as the actuator redundancy resulting from bi-articular actuation in robot arms [6], a closed-form solution based on the infinity norm is possible, and its higher performances in respect to the 2 norm in terms of output maximization have been shown [7], [8].

In this work, lateral dynamic control for EV is considered. A closed-form solution based on the ∞ norm for the 2 outputs to 3 inputs control allocation problem in EV lateral dynamic control is derived, and its higher performances in respect to the traditional 2 norm based algorithm are investigated.

In Sec. II the vehicle lateral dynamics modeling and allocation problem is described. In Sec. III the traditional 2 norm based and the proposed ∞ norm based models for resolving the 2 to 3 allocation problem are shown. In Sec. IV the simulation results are analyzed and discussed. Finally, the advantages of the proposed algorithm are summarized in Sec. V.

II. EV Lateral Dynamics Control

EVs offer apart from their particular energy source the opportunity to install in each wheel a motor, therefore introducing new degrees of freedom in the vehicle dynamic control design [9], [10]. In this contribution the opportunity to generate an additional yaw moment M_z by appropriate single wheel torque commands is exploited. Compared to conventional cars [11] the yaw moment M_z can be generated quite easily by a EV with In-Wheel-Motors. Additionally, it is assumed that front and rear steering are active, meaning that front and rear steering are influenced by the control system and are not strictly coupled with handwheel steering angle. Such vehicles do already exist as test vehicle in laboratories [12].

A. Vehicle lateral dynamics modelling

The linear bicycle model in the case of an In-Wheel-Driven Electric Vehicle with Active Front and Rear steering in the case of constant vehicle longitudinal velocity v_x (As far as the influence of longitudinal forces in contributing to the overall lateral forces due to the steering angle is concerned, we consider this influence as model uncertainty.) is as follows [13]:

$$\begin{aligned}
\dot{\mathbf{x}} &= \mathbf{A}\mathbf{x} + \mathbf{v}^* = \mathbf{A}\mathbf{x} + \mathbf{B}\mathbf{u}^* \\
\begin{bmatrix} \dot{\beta} \\ \dot{\gamma} \end{bmatrix} &= \begin{bmatrix} \frac{-(C_f+C_r)}{mv_x} & \frac{l_rC_r-l_fC_f}{mv_x^2}-1 \\ \frac{l_rC_r-l_fC_f}{J_z} & -\frac{l_r^2C_r+l_f^2C_f}{J_zv_x} \end{bmatrix} \begin{bmatrix} \beta \\ \gamma \end{bmatrix} + \\
&+ \begin{bmatrix} \frac{C_f}{mv_x} & \frac{C_r}{mv_x} & 0 \\ \frac{l_fC_f}{J_z} & -\frac{l_rC_r}{J_z} & \frac{1}{J_z} \end{bmatrix} \begin{bmatrix} \delta_f \\ \delta_r \\ M_z \end{bmatrix},
\end{aligned} \tag{1}$$

where C_f, C_r are the front and rear cornering stiffness values, m, J_z the vehicle mass and the vehicle yaw inertia, l_f, l_r the distance from the front and rear axle to the center of gravity and δ_f, δ_r, M_z the front steering angle,the rear steering angle and the additional yaw moment respectively. Three inputs are used to determine the two states (body slip angle β and yaw

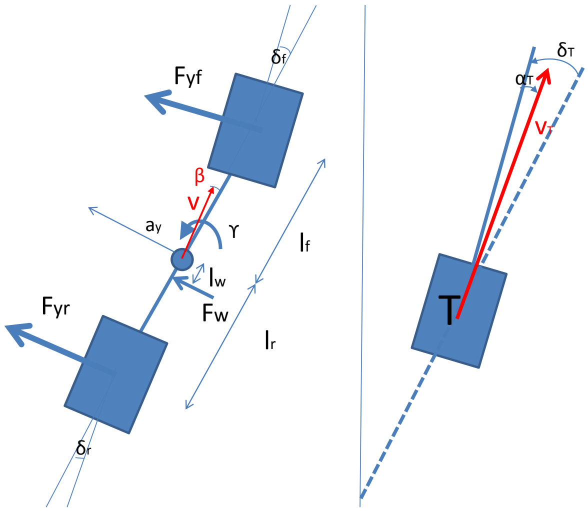

Fig. 1. Bicycle model (left) with combined front lateral and rear lateral tire forces and definition of tire slip angle α (right). (a_y: lateral acceleration, γ: yaw rate, β: body slip angle, δ_f: front steering angle, δ_r: rear steering angle, F_{yf}: combined front lateral tire force, F_{yr}: combined rear lateral tire force, F_w: wind disturbance force, l_f: distance of front axle from COG, l_r: distance of rear axle from COG , l_w: distance of aerocenter from COG).

rate γ). This means it is an over actuated system and control allocation problem of the type 2 to 3.

The model (1) describes the vehicle in the linear domain of operation. It assumes that the steering angles δ_f, δ_r and the tire slip angles α_f, α_r are small. However under certain operation condition the EV enters the non linear domain of operation. The allocation scheme should help to keep the EV in the linear domain of operation.

B. Vehicle lateral dynamics control and allocation problem

A control system for lateral vehicle dynamics is established as shown in Fig. 2. The controller tries to track the yaw rate γ and the body slip angle β of the vehicle. It is assumed that these two quantities are measured/observed. This may be difficult as far as the body slip angle β is concerned. However, this estimation problem is not part of this contribution, we refer to [14]. The controller computes a two dimensional virtual controller output $\mathbf{v}^*$ which is mapped by using an infinity norm criteria and the allocation equation to a three dimensional actuator demand $\mathbf{u}^*$ (true controller output) :

$$\mathbf{v}^* = \mathbf{B}\mathbf{u}^* \tag{2}$$

with

$$\mathbf{B} = \begin{bmatrix} \frac{C_f}{mv_x} & \frac{C_r}{mv_x} & 0 \\ \frac{C_f l_f}{J_z} & \frac{-C_r l_r}{J_z} & \frac{1}{J_z} \end{bmatrix}, \mathbf{u}^* = \begin{bmatrix} \delta_f \\ \delta_r \\ M_z \end{bmatrix}. \tag{3}$$

In the following we assume a linear relationship between the tire slip angles α_f, α_r and the steering angles δ_f, δ_r as follows:

$$\alpha_f = \delta_f - \beta - \frac{l_f}{v_x}\gamma \tag{4}$$

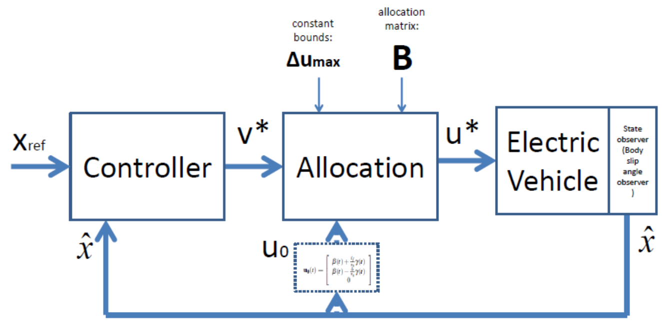

Fig. 2. Overview of the considered control system. The controller computes a virtual control input which is translated by the control allocator to the true control input. It is assumed that the vehicle yaw rate γ and the body slip angle β can be measured or observed.

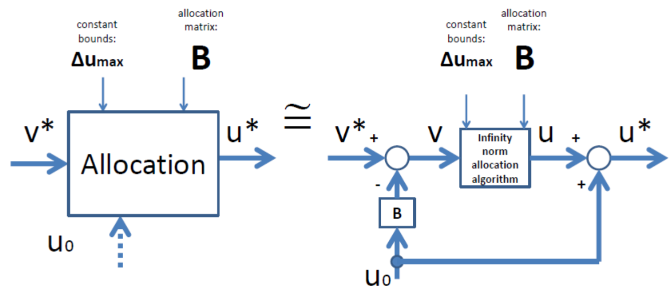

Fig. 3. Instead of allocating the front and rear steering angles directly, the allocator output u_1, u_2 are the front and rear tire slip angles which are translated to the steering angles. By doing so the bounds in the allocation can be kept constant.

$$\alpha_r = \delta_r - \beta + \frac{l_r}{v_x}\gamma \tag{5}$$

Since the value of the tire slip angles α_f, α_r are to be kept small and not necessarily the steering angles δ_f, δ_r in order to keep the vehicle in the linear range of operation (stable) and in order to avoid time variant bounds as maximal values in the allocation equation we decompose the allocated variable (actuator demand):

$$\mathbf{u}^* = \mathbf{u}_0 + \mathbf{u}, \tag{6}$$

where $\mathbf{u_0}$ corresponds to the actuator demand corresponding to zero tire slip angles:

$$\mathbf{u_0}(t) = \begin{bmatrix} \beta(t) + \frac{l_f}{v_x}\gamma(t) \\ \beta(t) - \frac{l_r}{v_x}\gamma(t) \\ 0 \end{bmatrix}. \tag{7}$$

With the decomposition (Fig. 3) of the actuator demand the allocation problem is formulated as following:

$$\mathbf{v} = \mathbf{B}\mathbf{u}. \tag{8}$$

By combining (2), (6) and (8) it follows:

$$\mathbf{v} = \mathbf{v}^* - \mathbf{B}\mathbf{u}_0. \tag{9}$$

The entry u_1 and u_2 of the vector $\mathbf{u} = [u_1, u_2, u_3]^T$ can be directly interpreted as the front and rear lateral tire slip angle α_f, α_r respectively.

Taking into account (8), given $\mathbf{u}$ it is possible to determine $\mathbf{v}$ uniquely. On the other hand, given $\mathbf{v}$ it is generally not possible to determine uniquely $\mathbf{u}$ due to the actuator redundancy. The problem represented by (8) is referred in the following as 2 outputs to 3 inputs control allocation problem. The vector $\mathbf{u} = [u_1, u_2, u_3]^T$ in this contribution is also referred as true controller output and the vector $\mathbf{v} = [v_1, v_2]^T$ as virtual controller output and

$$\mathbf{B} = \begin{bmatrix} b_{11} & b_{12} & b_{13} \\ b_{21} & b_{22} & b_{23} \end{bmatrix} \tag{10}$$

as allocation matrix.

III. 2 OUTPUTS TO 3 INPUTS ALLOCATION RESOLUTION

To determine a specific solution from the infinite number of solutions due to the actuation redundancy an optimization criteria must be used. The most used criteria is the (weighted) least square problem (2 norm), mainly because the solution is expressed by a closed-form expression (using the pseudo inverse). However, the least square solution does not exploit the available actuation range very well [6]. In contrast, optimization criteria based on ∞ norm allow the use of all the solution space, but usually the solution is determined using iterative algorithms. As a consequence, to have a closed-form solution based on the ∞ norm is highly advantageous.

A. 2 norm based approach

The 2 to 3 allocation problem is resolved using the 2 norm by solving the following problem:

$$\begin{aligned} \min \quad & \sqrt{\frac{(u_1)^2}{(u_1^m)^2} + \frac{(u_2)^2}{(u_2^m)^2} + \frac{(u_3)^2}{(u_3^m)^2}} \\ \text{s.t.} \quad & \mathbf{v} = \mathbf{B}\mathbf{u} \end{aligned} \tag{11}$$

The solution of the problem expressed by (11) is obtained using a generalized pseudo inverse:

$$\mathbf{u}_{opt} = \mathbf{W}^{-1}\mathbf{B}^T(\mathbf{B}\mathbf{W}^{-1}\mathbf{B}^T)^{-1}\mathbf{v} \tag{12}$$

where

$$\mathbf{W} = diag(\frac{1}{(u_1^m)^2}, \frac{1}{(u_2^m)^2}, \frac{1}{(u_3^m)^2}). \tag{13}$$

B. Infinity norm based approach

The 2 to 3 allocation problem is resolved using the ∞ norm by solving the following problem:

$$\begin{aligned} \min \quad & \max\left(\frac{|u_1|}{u_1^m}, \frac{|u_2|}{u_2^m}, \frac{|u_3|}{u_3^m}\right) \\ \text{s.t.} \quad & \mathbf{v} = \mathbf{B}\mathbf{u} \end{aligned} \tag{14}$$

The objective function is weighted, that is the three input values u_i for $(i = 1, 2, 3)$ are scaled by the respective maximum value u_i^m for $(i = 1, 2, 3)$. By doing so the entire solution space

$$-u_i^m \leq u_i \leq u_i^m, \text{ for } i = 1, 2, 3 \tag{15}$$

is exploited efficiently as shown in III-C.

A closed form solution of the problem (14) is represented by three functions, each one expressed with a three piecewise linear function:

$$u_1 = \begin{cases} \frac{v_1 b_{23} u_1^m - v_2 b_{13} u_1^m}{u_1^m det_{13} + u_2^m det_{23}} & \text{if } case_1 \\ \frac{v_1 b_{22} u_1^m - v_2 b_{12} u_1^m}{u_1^m det_{12} - u_3^m det_{23}} & \text{if } case_2 \\ \frac{-v_1(b_{22}u_2^m - b_{23}u_3^m) - v_2(b_{13}u_3^m - b_{12}u_2^m)}{u_3^m det_{13} - u_2^m det_{12}} & \text{if } case_3 \end{cases} \tag{16}$$

$$u_2 = \begin{cases} \frac{v_1 b_{23} u_2^m - v_2 b_{13} u_2^m}{u_1^m det_{13} + u_2^m det_{23}} & \text{if } case_1 \\ \frac{-v_1(b_{21}u_1^m + b_{23}u_3^m) + v_2(b_{11}u_1^m + b_{13}u_3^m)}{u_1^m det_{12} - u_3^m det_{23}} & \text{if } case_2 \\ \frac{-v_1 b_{21} u_2^m + v_2 b_{11} u_2^m}{u_2^m det_{12} - u_3^m det_{13}} & \text{if } case_3 \end{cases} \tag{17}$$

$$u_3 = \begin{cases} \frac{-v_1(b_{21}u_1^m + b_{22}u_2^m) + v_2(b_{11}u_1^m + b_{12}u_2^m)}{u_1^m det_{13} + u_2^m det_{23}} & \text{if } case_1 \\ \frac{v_1 b_{22} u_3^m - v_2 b_{12} u_3^m}{u_1^m det_{12} - u_3^m det_{23}} & \text{if } case_2 \\ \frac{v_1 b_{21} u_3^m - v_2 b_{11} u_3^m}{u_2^m det_{12} - u_3^m det_{13}} & \text{if } case_3 \end{cases} \tag{18}$$

where

$$det_{23} = b_{12}b_{23} - b_{13}b_{22} \tag{19}$$

$$det_{13} = b_{11}b_{23} - b_{13}b_{21} \tag{20}$$

$$det_{12} = b_{11}b_{22} - b_{12}b_{21} \tag{21}$$

and

$$\begin{aligned} case_1 =& (kv_{21}v_2 \leq kv_{11}v_1 \text{ and } kv_{22}v_2 \geq kv_{12}v_1) \text{ or} \\ & (kv_{21}v_2 \geq kv_{11}v_1 \text{ and } kv_{22}v_2 \leq kv_{12}v_1) \\ case_2 =& (kv_{21}v_2 \leq kv_{11}v_1 \text{ and } kv_{23}v_2 \geq kv_{13}v_1) \text{ or} \\ & (kv_{21}v_2 \geq kv_{11}v_1 \text{ and } kv_{23}v_2 \leq kv_{13}v_1) \\ case_3 =& (kv_{22}v_2 \leq kv_{12}v_1 \text{ and } kv_{23}v_2 \leq kv_{13}v_1) \text{ or} \\ & (kv_{22}v_2 \geq kv_{12}v_1 \text{ and } kv_{23}v_2 \geq kv_{13}v_1) \end{aligned}$$

where

$$kv_{11} = (b_{21}u_1^m + b_{22}u_2^m + b_{23}u_3^m) \tag{22}$$

$$kv_{12} = (b_{21}u_1^m + b_{22}u_2^m - b_{23}u_3^m) \tag{23}$$

$$kv_{13} = (b_{21}u_1^m - b_{22}u_2^m + b_{23}u_3^m) \tag{24}$$

$$kv_{21} = (b_{11}u_1^m + b_{12}u_2^m + b_{13}u_3^m) \tag{25}$$

$$kv_{22} = (b_{11}u_1^m + b_{12}u_2^m - b_{13}u_3^m) \tag{26}$$

$$kv_{23} = (b_{11}u_1^m - b_{12}u_2^m + b_{13}u_3^m) \tag{27}$$

Equations (16), (17), and (18) are derived following the same method used in [6]. They are continuous in all the domain $D = (v_1, v_2)$ under the condition that all the denominators are different from 0 (satisfied for $\boldsymbol{B}$ and $\boldsymbol{u}^m$ in this work).

C. Infinity Norm Approach: the Reason Why

Fig. 4 shows the graphical comparison between ∞ norm and 2 norm optimization criteria in selecting the optimal solution for a problem in $\mathbb{R}^2$. The dashed line represents the infinite set of solutions (x, y) that satisfy,

$$k = \alpha x + y \tag{28}$$

where α represents the relationship between the desired output k and the necessary inputs x and y. The positive constants x^{max}

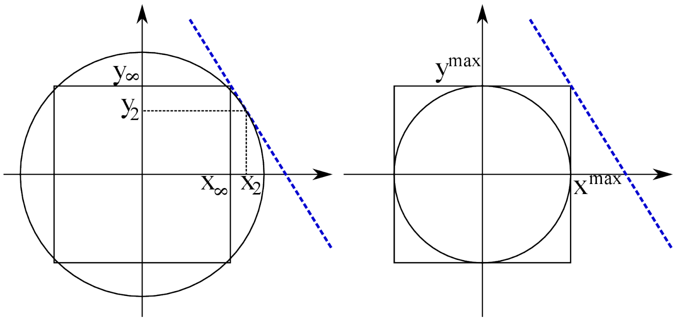

Fig. 4. Graphical comparison between ∞ norm and 2 norm: solution comparison (left), no solution for 2 norm (right)

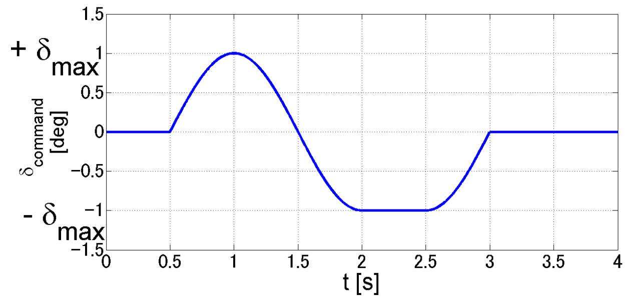

Fig. 5. Steering command signal δ_{steer} "sine with a dwell" used for the simulation series. The maximal steering angle δ_{max} is varied during the simulation runs.

and y^{max} define the allowable ranges for x and y:

$$-x^{max} \leq x \leq x^{max} \tag{29}$$

$$-y^{max} \leq y \leq y^{max} \tag{30}$$

The two sets (x_2, y_2) and (x_∞, y_∞) in Fig. 4 (left) are the two solutions of (28) calculated using the 2 norm (the circle) and ∞ norm (the square) optimization criteria, respectively. By definition, the infinity norm minimize the maximum input, therefore it holds:

$$\max\{|x_\infty|, |y_\infty|\} \leq \max\{|x_2|, |y_2|\} \tag{31}$$

Therefore, if x and y are bounded as in (29) and (30), the ∞ norm model admits solution for higher values of k than the 2 norm, as shown in Fig. 4 (right). The greater solution space of the ∞ norm model holds also in $\mathbb{R}^3$, the mathematical space of the redundancy resolution problem in this work.

IV. Simulation and Results

Advantages by using the ∞ norm are now shown by considering an EV at constant velocity carrying out a "sine with a dwell" steering command. The simulation runs have been carried out with the professional simulation environment CarSim. A highly sophisticated CarSim vehicle model has been used that considers explicitly the different side slip angles at the four wheels, load transfer, suspension effects and a complex non linear tyre model including tire dynamics. Whereas the control design has been based on a highly simplified model of the vehicle dynamics as shown in (1), the overall system simulation used the aforementioned sophisticated CarSim vehicle model. The parameters are set in the following way: mass $m = 830\ kg$, yaw inertia $Jz = 562\ kgm^2$ and front (rear) axle distance from the center of gravity $l_f = 0.999\ m$ ($l_r = 0.701\ m$) has been considered. The vehicle is assumed to be running on a slightly slippery road with $\mu = 0.7$ and the driver to give a sine with a dwell steering command as depicted in Fig. 5.

As controller a sliding mode controller as described in [4] has been used, the controller parameter (gains) have been set once and left untouched during all simulation runs. The controller gets reference values which are derived from the "sine with a dwell" steering command:

$$\gamma_{ref} = \frac{v_x}{(l_f + lr)(1 + \frac{v_x^2}{v_{ch}^2})}\delta_{steer} \tag{32}$$

where v_{ch} is the characteristic velocity of the car. The reference for the body slip angle has been set to zero, $\beta_{ref} = 0°$.

Two allocation methods have been compared. The first is the weighted means square solution according to (11) and the second one is the weighted infinity norm according to (14) with the closed form solution as described in III-B. Both methods have been embedded in the scheme of Fig. 3 where the tire slip angles α_f, α_r are allocated by the allocation algorithm instead of the steering angles and after the allocation translated to the steering angles δ_f, δ_r by use of (4), (5) and (6) since the body slip angle β, the yaw rate γ and the velocity v_x are assumed to be known. The torque moment M_z has been evenly distributed to the 4 wheels. The tire slip angle maximal values u_1^m, u_2^m have been set to 5° for front and rear tire slip. The torque moment value u_3^m has been set to 2000 Nm. Without further knowledge of these bounds this seems to be reasonable. The inclusion of online estimation of these bounds is not topic of this contribution, it is referred to [15], [16], [17]. Additionally geometric constraints for the steering angles have been considered in the simulation ($\delta_{f,max} = 17°, \delta_{r,max} = 4.5°$).

In Fig. 6 and Fig. 7 the steering manoeuvre from Fig. 5 with two different maximum steering angles δ_{max} is shown in detail. In Fig. 6 ($\delta_{max} = 3°, v_x = 70km/h$) both approaches (2 and ∞ norm) satisfactorily achieve the desired lateral dynamics. The yaw rate tracking error is negligible and the body slip angle kept small. This situation changes (Fig. 7) if the steering angle of the same manoeuvre is slightly increased ($\delta_{max} = 3.25°, v_x = 70km/h$). In this case the allocation efficiency (by allocation efficiency we understand the exploitation of the available solution space according to (15)) of the ∞ norm approach prevents the controller to reach the actuator saturation. In the case of 2 norm approach the actuator limitations are reached and the controller has difficulties to keep the yaw rate tracking error and the body slip angle small leading to some inaccuracy in the yaw rate tracking and a pronounced body slip angle (1.36°) compared to a negligible body slip angle of 0.18° in the case of ∞ norm approach. In Fig. 8 the tire slip angles α_f, α_r are compared. It can be seen that the allocation is

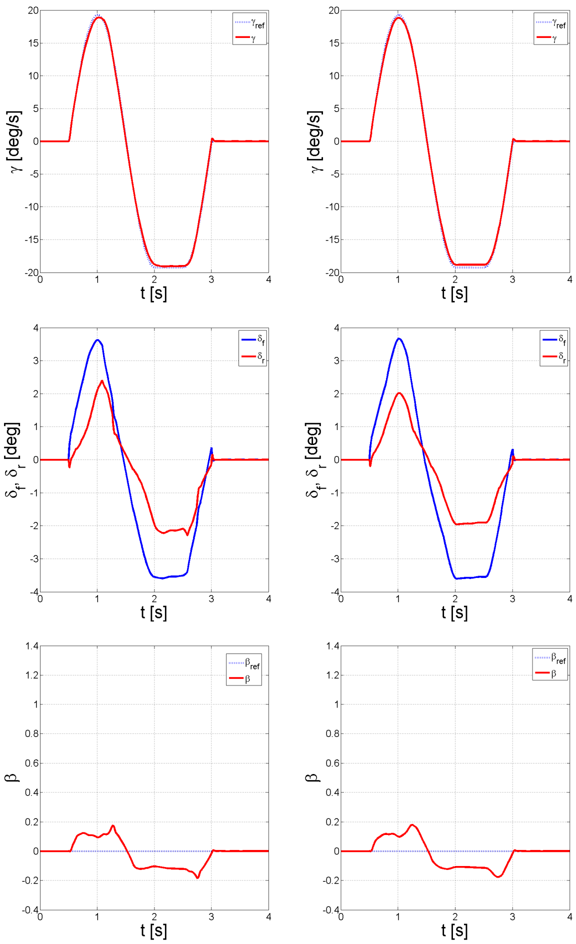

Fig. 6. Comparison between 2 norm (left) and ∞ norm (right) allocation approach at a speed of $70 km/h$ and with maximum steering command $\delta_{max} = 3°$. The diagram show the yaw rate (top), front and rear steering angle (middle) and achieved body slip angle (bottom).

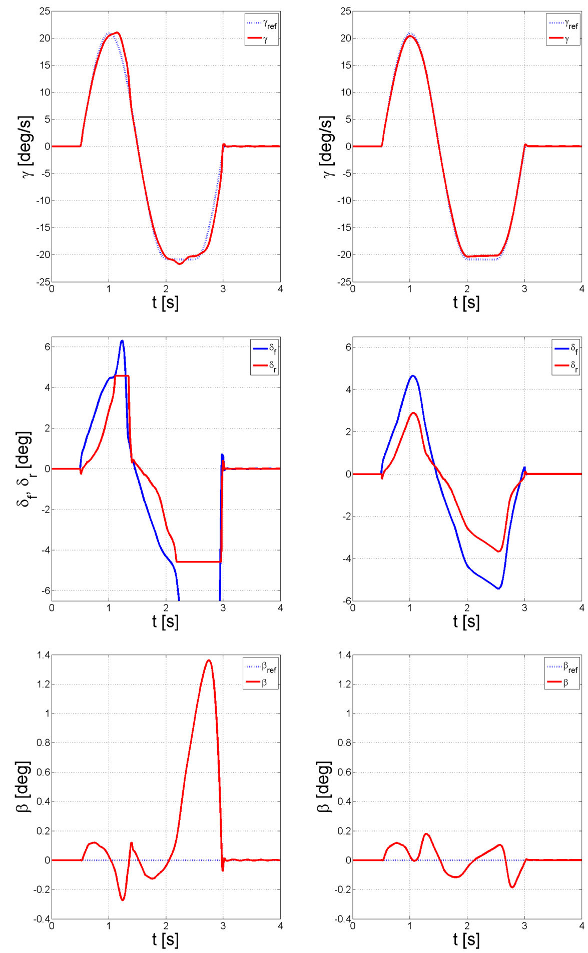

Fig. 7. Comparison between 2 norm (left) and ∞ norm (right) allocation approach at a speed of $70 km/h$ and with maximum steering command $\delta_{max} = 3.25°$. The diagram show the yaw rate (top), front and rear steering angle (middle) and achieved body slip angle (bottom).

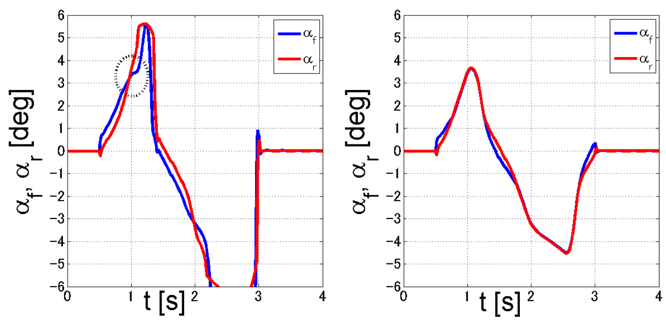

Fig. 8. Allocated front and rear tire slip angles α_f, α_r comparison between 2 norm (left) and ∞ norm (right) allocation approach at a speed of $70 km/h$ and with maximum steering command $\delta_{max} = 3.25°$. Due do the different allocation strategy, the 2 norm leads to the violation of the bounds (5°).

different especially after 1 s and that the 2 norm allocation violates the 5° bound meaning that the vehicle becomes highly non linear which has drastic consequences for the dynamics control system. During the "dwell" period of the manoeuvre the steering actuators saturate.

The overall results are summarized in Tab. I and Tab. II. For both the 2 and the ∞ norm allocation, the velocity has been varied from $60 km/h$ to $90 km/h$ and the maximum steering angle from 2° to 4.5°. The steering angle command is shown in Fig. 5. It is translated by (32) into an yaw rate reference value for the controller. In Tab. I the RMS value of the yaw rate tracking error is shown. It is important to track the yaw rate very precisely in order to have a high performance lateral vehicle dynamics. Tab. II shows the maximal body slip angle occurring during the manoeuvre. A high body slip angle is undesired, dangerous, and should be avoided. For low velocities and small steering angles 2 norm and ∞ norm allocation behave equally well. For higher velocities and steering angles the ∞ norm is superior. Actuator saturation occurs later (shown with italic numbers) and the body slip angle is quite reduced compared to the 2 norm solution. For certain combinations of velocity and steering angle the vehicle gets unstable (marked with $*$). It is a consequence of the vehicle running into the highly non linear mode of operation due to lateral tire force saturation and/or actuator physical saturation. The ∞ norm approach due to its allocation efficiency enlarges the operation range where the vehicle is not

speed	δ_{max}	2°	2.25°	2.5°	2.75°	3°	3.25°	3.5°	3.75°	4°	4.25°	4.5°
60 km/h	**2 norm**	0.16	0.18	0.19	0.20	0.21	0.22	0.22	*0.56*	*0.95*	*1.24*	*2.29*
	∞ norm	0.17	0.19	0.19	0.20	0.21	0.21	0.22	0.23	*0.47*	*0.80*	*1.09*
70 km/h	**2 norm**	0.18	0.20	0.21	0.21	0.21	*0.75*	*1.10*	*	*	*	*
	∞ norm	0.19	0.20	0.20	0.21	0.21	0.26	*0.72*	*1.05*	*1.42*	*1.99*	*2.72*
80 km/h	**2 norm**	0.20	0.20	0.20	*0.49*	*0.94*	*	*	*	*	*	*
	∞ norm	0.20	0.20	0.21	0.22	*0.62*	*0.98*	*1.38*	*1.93*	*2.66*	*3.67*	*
90 km/h	**2 norm**	0.20	0.19	*0.57*	*0.99*	*	*	*	*	*	*	*
	∞ norm	0.20	0.20	0.23	*0.69*	*1.07*	*1.49*	*2.06*	*2.88*	*	*	*

TABLE I

RMS VALUE OF THE YAW TRACKING ERROR $\Delta\gamma = \gamma_{ref} - \gamma$ IN $\frac{\circ}{s}$ FOR THE "SINE WITH A DWELL" STEERING COMMAND FOR DIFFERENT MAXIMUM STEERING ANGLES AND DIFFERENT SPEEDS. * MEANS THAT THE VEHICLE BECOMES UNSTABLE, *Italic* NUMBERS MEAN THAT THE ACTUATOR SOMETIMES SATURATE DURING THE MANOEUVRE.

speed	δ_{max}	2°	2.25°	2.5°	2.75°	3°	3.25°	3.5°	3.75°	4°	4.25°	4.5°
60 km/h	**2 norm**	0.15	0.16	0.16	0.17	0.18	0.21	0.20	*0.39*	*2.37*	*3.91*	*6.73*
	∞ norm	0.14	0.16	0.17	0.18	0.19	0.20	0.21	0.21	*1.11*	*2.12*	*2.92*
70 km/h	**2 norm**	0.14	0.14	0.16	0.18	0.18	*1.36*	*3.13*	*	*	*	*
	∞ norm	0.14	0.15	0.16	0.17	0.18	0.18	*1.57*	*2.36*	*3.19*	*3.87*	*4.05*
80 km/h	**2 norm**	0.13	0.14	0.16	*0.73*	*2.35*	*	*	*	*	*	*
	∞ norm	0.13	0.14	0.15	0.16	*1.11*	*1.90*	*2.67*	*3.36*	*3.53*	*3.76*	*
90 km/h	**2 norm**	0.12	0.15	*0.72*	*2.45*	*	*	*	*	*	*	*
	∞ norm	0.13	0.14	0.14	*1.09*	*1.81*	*2.54*	*2.95*	*3.17*	*	*	*

TABLE II

MAXIMUM BODY SLIP ANGLE β IN ° FOR THE "SINE WITH A DWELL" STEERING COMMAND FOR DIFFERENT MAXIMUM STEERING ANGLES AND DIFFERENT SPEEDS. * MEANS THAT THE VEHICLE BECOMES UNSTABLE, *Italic* NUMBERS MEAN THAT THE ACTUATOR SOMETIMES SATURATE DURING THE MANOEUVRE.

yet into the heavy non linear region. However, if especially due to bad road condition and too high velocity and/or large steering angles with regard to the μ value of the road the controller demand cannot be realized, the reference signal should be adapted.

V. CONCLUSIONS AND OUTLOOK

In this work a new approach to solve the 2 to 3 control allocation problem in EV lateral dynamic control is proposed. The algorithm is based on the infinity norm and a closed-form solution for the specific problem of EV lateral dynamic control is derived. The solution is implemented with a defined low number of arithmetic and logic operations. In contrast to the 2 norm approach, when using the proposed algorithm the linear region in which the EV operates is extended, the actuator saturation occurs at higher velocity, the body slip angle at high velocities is significantly reduced, the maximum velocity at which the EV shows instability is increased. Further research will be to consider each wheel of the IWM driven EV separately. Together with the steering actuators (front and rear), 6 actuators must be controlled. Depending how many vehicle dynamics output variables should be controlled it could be a (3 to 6), (4 to 6), or (5 to 6) allocation problem. A specific closed form solution based on infinity norm for such higher dimensional problems will be investigated.

REFERENCES

[1] O. Härkegård, *Backstepping and Control Allocation with Applications to Flight Control.*, PhD Thesis, Dept. of Electr. Eng., Linköping Univ., 2003.

[2] V. Salvucci, Y. Kimura, S. Oh, and Y. Hori, *Non-Linear Phase Different Control for Precise Output Force of Bi-Articularly Actuated Manipulators*, Advanced Robotics, 2013.

[3] Y. Chen and J. Wang, *Energy-Efficient Control Allocation with Applications on Planar Motion Control of Electric Ground Vehicles*, American Control Conference, pp. 2719 - 2724, 2011.

[4] A. Viehweider and Y. Hori, *Electric Vehicle Lateral Dynamics Control based on Instantaneous Cornering Stiffness Estimation and an Efficient Allocation Scheme*, MATHMOD, Conference on Mathematical Modelling, pp. 1-6, 2012.

[5] N. Ando and H. Fujimoto, *Yaw-rate control for electric vehicle with active front/rear steering and driving/braking force distribution of rear wheels*, Adv. Motion Control, 11th IEEE Int. Workshop on, pp. 726-731, 2010.

[6] V. Salvucci, Y. Kimura, S. Oh, and Y. Hori, *Force maximization of bi-articular actuated manipulators using infinity norm*, IEEE/ASME Transaction on Mechatronics, 2013.

[7] V. Salvucci, Y. Kimura, S. Oh, and Y. Hori, *Experimental verification of infinity norm approach for force maximization of manipulators driven by bi-articular actuators*, ACC, pp. 4105–4110, 2011.

[8] V. Salvucci, Y. Kimura, S. Oh, T. Koseki, and Y. Hori, *Comparing Approaches for Actuator Redundancy Resolution in Bi-articularly Actuated Robot Arms*, IEEE/ASME Transactions on Mechatronics, 2013.

[9] Y. Hori, *Future Vehicle Driven by Electricity and Control*, IEEE Transactions on Industrial Electronics, Vol. 51, No. 5, October 2004.

[10] E. Katusyama, *Decoupled 3D moment control using in-wheel motors*, Vehicle System Dynamics, pp. 1-14, 2012.

[11] D. Bianchi, A. Borri, G. Burgio, M.D. Di Benedetto, S. Di Gennaro, *Adaptive integrated vehicle control using active front steering and rear torque vectoring*, CDC/CCC, pp. 3557 - 3562, 2009.

[12] H. Fujimoto, *E-motion*, *http://www.dspace.com*, Dspace magazine, No. 1, pp.16-19, 2009.

[13] H. B. Pacejka, *Tyre and Vehicle Dynamics*, Elsevier, 2006.

[14] C. Geng, T. Uchida and Y. Hori, *Body Slip Angle Estimation and Control for Electric Vehicle with In-Wheel Motors*, IECON 2007, pp. 1-6, 2007.

[15] L. Haffner, M. Kozek, J. Shi and H. P. Joergl, *Estimation of the maximum friction coefficient for a passenger vehicle using the instantaneous cornering stiffness*, American Control Conference, pp. 4591-4596, 2008.

[16] A. Viehweider, K. Nam, H. Fujimoto, Y. Hori, *Evaluation of a Betaless Instantaneous Cornering Stiffness Estimation Scheme for Electric Vehicles*, REM Mechatronics, pp. 1–8, 2012.

[17] A. Viehweider et al., *Electric Vehicle Dynamics Modelling considering Tire Force Bounds for Efficient Allocation*, Mathematical and Computer Modelling of Dynamical Systems, in preparation.